



Article

# Investigating Sustainability Index, $^{99}\text{Mo}$ Output and $^{239}\text{Pu}$ Levels in $\text{UO}_2$ Targets by Substituting $^{238}\text{U}$ with Ce

Robert Raposio <sup>1,2,\*</sup>, Anatoly Rosenfeld <sup>2</sup>, Juniper Bedwell-Wilson <sup>1</sup> and Gordon Thorogood <sup>1</sup>

<sup>1</sup> Australian Nuclear Science and Technology Organisation, Lucas Heights, NSW 2234, Australia

<sup>2</sup> Centre for Medical Radiation Physics, University of Wollongong, Wollongong, NSW 2500, Australia

\* Correspondence: rra@ansto.gov.au

**Abstract:** A new target material combination was modelled to replace the existing uranium-aluminium design used for  $^{99}\text{Mo}$  manufacture to increase the sustainability of the production process. Previous efforts to develop a more sustainable uranium target for  $^{99}\text{Mo}$  production, resulted in the levels of  $^{239}\text{Pu}$  in the target after irradiation being elevated due to the increase in  $^{238}\text{U}$  present. MCNP6.2 was used to model 4 different cylindrical targets based on 4–7 days irradiation to further understand this effect. To reduce the resultant  $^{239}\text{Pu}$  levels, ratios of 0–99% of Ce were used as a replacement for  $^{238}\text{U}$ . The results show that the addition of  $^{140}\text{Ce}$  and the removal of  $^{238}\text{U}$  reduced the  $^{239}\text{Pu}$  levels in the target significantly thus increasing the sustainability of the target and giving a slight increase to the  $^{99}\text{Mo}$  output of the targets.

**Keywords:** MCNP6 modelling;  $^{99}\text{Mo}$  manufacturing; sustainable manufacturing



**Citation:** Raposio, R.; Rosenfeld, A.; Bedwell-Wilson, J.; Thorogood, G. Investigating Sustainability Index,  $^{99}\text{Mo}$  Output and  $^{239}\text{Pu}$  Levels in  $\text{UO}_2$  Targets by Substituting  $^{238}\text{U}$  with Ce. *J. Nucl. Eng.* **2022**, *3*, 295–305. <https://doi.org/10.3390/jne3040017>

Academic Editor: Shichang Liu

Received: 30 August 2022

Accepted: 17 October 2022

Published: 26 October 2022

**Publisher's Note:** MDPI stays neutral with regard to jurisdictional claims in published maps and institutional affiliations.



**Copyright:** © 2022 by the authors. Licensee MDPI, Basel, Switzerland. This article is an open access article distributed under the terms and conditions of the Creative Commons Attribution (CC BY) license (<https://creativecommons.org/licenses/by/4.0/>).

## 1. Introduction

In efforts to explore the development of a method for  $^{99}\text{Mo}$  production using fission of very low enriched to non-enriched uranium targets previous results have led to two main causes of concern:

- (1) Increased amounts of  $^{238}\text{U}$  waste compared to low-enriched uranium targets [1];
- (2) The higher amount of  $^{238}\text{U}$  in the target leads to increased amounts of  $^{239}\text{Pu}$  being produced per GBq of  $^{99}\text{Mo}$  produced which could be a cause for non-proliferation concerns [2–4].

Therefore, a potential downside of using 1% enriched uranium targets which have a high sustainability index is that there is a lot of  $^{238}\text{U}$  that still present that would end up being combined with mixed fission products and so be considered as waste. Given that in the current enrichment process  $^{238}\text{U}$  is removed from natural uranium as a waste product, this  $^{238}\text{U}$  is not contaminated with other radioactive products and can be used in industry for useful applications such as radiation shielding, ballast for aircraft, and military uses [5].

A potential improvement for a sustainable target could potentially be to substitute some or most of the portion of  $^{238}\text{U}$  in the target for another material that has similar properties in terms of thermal conductivity, crystal structure and irradiation behaviour to  $^{238}\text{U}$  to reduce the amount of total uranium and plutonium waste in the spent target. A possible substitution for  $\text{UO}_2$  in the target could be  $\text{CeO}_2$  which has similar chemical, thermal and physical properties whilst undergoing no fission reaction [6–9].  $^{140}\text{Ce}$  has a thermal neutron cross section of  $0.59 \pm 0.06$  barns [10] and when  $^{140}\text{Ce}$  captures a neutron it transmutes to  $^{141}\text{Ce}$  which undergoes further beta decay to the stable  $^{141}\text{Pr}$  with a half-life of 32.508 days [11].  $\text{CeO}_2$  was found to have comparable thermophysical properties to  $\text{UO}_2$  below temperatures of 1673 K [12].

$\text{CeO}_2$  has been found to have a high chemical stability as well as thermal stability [13] which would make it suitable for use in a target structure.  $\text{CeO}_2$  and  $\text{UO}_2$  was mixed to create the stable compound  $2\text{CeO}_2 \cdot \text{UO}_2$  [14] and using solid state reactions uranium and

cerium can be synthesized into  $U_{1-x}Ce_xO_{2-\delta}$  where  $x$  ranges from 0 to 0.1 [15]. The mixing of  $UO_2$  and  $CeO_2$  was found to have nearly zero mixing enthalpies making it an ideal solid solution [16] and cerium was found to be soluble in  $UO_2$  [17]. Cerium dioxide has been used as a simulant for uranium dioxide to study radiation damage from a materials point of view [18–22]. Similarities in grain boundaries were found between  $UO_2$  and  $CeO_2$  indicating that from a radiation damage perspective, the addition of  $CeO_2$  to the target would not compromise target structure under irradiation conditions [23]. However, there are some small differences as it was found that the Ce in the  $CeO_2$  is more likely to be displaced under irradiation conditions than the U in the  $UO_2$  [24]. Furthermore, a comparison of the mechanical properties of  $CeO_2$  and  $UO_2$  such as swelling and cracking over temperature ranges showed that under irradiation conditions  $CeO_2$  is a suitable surrogate for a  $UO_2$  target [25–28].

In terms of production cost, cerium oxide has a price of approximately \$1150 USD per metric tonne [29] whereas the price of uranium oxide is expected to be around \$100,000 USD per tonne [30] therefore presenting a significant cost saving if a large portion of the targets are made from cerium oxide.

## 2. Materials and Methods

### 2.1. Varying amounts of $^{140}Ce$ and $^{238}U$ in the Target

The following simulations were performed using MCNP6.2 [31] and CINDER90. MCNP stands for Monte Carlo N-Particle and is a radiation transport code that simulates in 3 dimensions and can model 37 particle types for functions such as criticality, shielding or burnup for example. Monte Carlo radiation transport methods were developed in 1947 and widely used in Los Alamos National Laboratory (LANL) where the code underwent various evolutions until in 1977 MCNP was born. MCNP6 is the merger of MCNP5 and MCNPX and it can utilise the ENDF/B-VII.1 database for nuclide parameters [31]. MCNP6.2 can track different particle types over a large range of energies and is a general-purpose, continuous-energy, generalised geometry, time-dependant Monte Carlo radiation-transport code [31]. MCNP6.2 can be used with target geometry, materials and reactor conditions as inputs and outputs include fission product yields and burnup of uranium which are directly related to the aims of this thesis. MCNP is currently used in the  $^{99}Mo$  production industry for forecasting theoretical yields which is another reason it was chosen as the preferred software package to use for this thesis.

The reactor dimensions and target positioning in this paper were identical to the model reactor used previously [32–34] and a diagram of the model is shown in Figure 1. The main change in this study is the target material.  $^{140}CeO_2$  was added to the model for simplicity due to its 88.449% natural abundance [35] in increments of 10% with a corresponding reduction in the amount of  $^{238}U$  by the same percentage with a 1%  $^{235}U$  level maintained throughout. There is little difference in the thermal neutron absorption cross section of natural Ce (0.63) with that of  $^{140}Ce$  (0.59). Table 1 shows the parameters used.

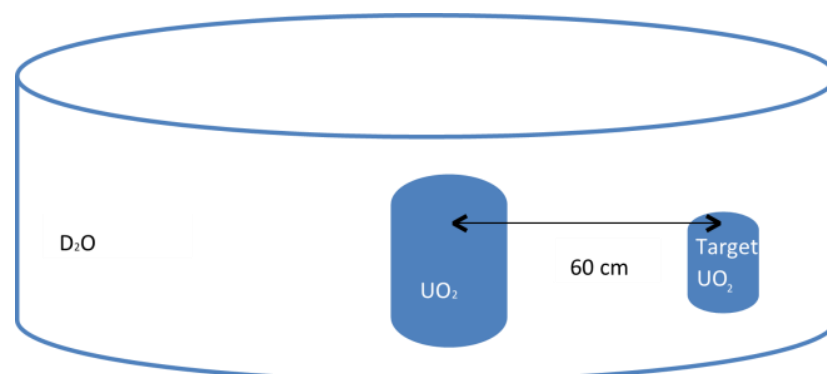


Figure 1. Visual representation of reactor model to show target location.

**Table 1.** Material compositions of targets.

Ce in Target (%)	<sup>235</sup> U in Target (%)	<sup>238</sup> U in Target (%)
0	1	99
10	1	89
20	1	79
30	1	69
40	1	59
50	1	49
60	1	39
70	1	29
80	1	19
90	1	9
99	1	0

### 2.2. Sustainability Index

As defined in Raposio (in press) [32], a simplistic way to describe the current methods of production are based upon the following formula which gives the amount of saleable product from a scheduling point of view:

$$\text{Output} = \frac{{}^{99}\text{Mo (GBq)}}{\text{Time (weeks)}} \tag{1}$$

To achieve a high output from a target design perspective it is necessary to consider the following factors: uranium density, mass, flux at irradiated position, reactivity worth, heat flux, total heat as well as accident analysis. When considering uranium density and mass to produce a high output it is logical to pack as much <sup>235</sup>U into the target as possible to ensure the maximum number of total fissions per unit time. In this case, the <sup>235</sup>U is in a state of saturation as there is significantly greater quantities present in the target than will ever fission in a short amount of time in a reactor.

An argument for the proposed alternative “lower waste” method could look like this: <sup>99</sup>Mo target efficiency ( $\epsilon_{\text{targ}}$ ) could be stated as the amount of activity of <sup>99</sup>Mo produced per gram of <sup>235</sup>U initially present in the target:

$$\epsilon_{\text{targ}} = \frac{{}^{99}\text{Mo produced (GBq)}}{{}^{235}\text{U in target (g)}} = \frac{A_T ({}^{99}\text{Mo})}{m_T ({}^{235}\text{U})} \tag{2}$$

Additionally, the efficiency of a <sup>99</sup>Mo target in terms of waste minimisation may also be expressed as the amount of activity produced per gram of <sup>235</sup>U burned up, or <sup>235</sup>U<sub>b</sub>, rather than—as discussed above—per gram of <sup>235</sup>U initially in the target. Hence:

$$\begin{aligned} \epsilon'_{\text{targ}} &= \frac{{}^{99}\text{Mo produced (GBq)}}{{}^{235}\text{U}_b \text{ (g)}} \\ &= \frac{A_T \text{ (GBq)}}{{}^{235}\text{U}_b \text{ (g)}} \end{aligned} \tag{3}$$

An important point is that the target efficiency is not absolute and will behave differently under different irradiation conditions such as flux and irradiation time and thus target efficiency needs to be optimised for the typical irradiation conditions it will experience. <sup>99</sup>Mo target efficiency when used in isolation would lead to poor target design if it were hypothetically taken to its extreme. A target of 100 atoms of <sup>235</sup>U would be highly efficient given the extremely high probability of all the 100 atoms fissioning to produce approximately 6 atoms of <sup>99</sup>Mo which is of no use to a <sup>99</sup>Mo producer who is used to dealing with activities in the GBq range. Therefore, an efficient target would be one that minimises the amount of <sup>235</sup>U needed to produce the required activity of <sup>99</sup>Mo to satisfy customer demand and would lead to minimisation of waste. A highly efficient target however does not consider the additional requirement of <sup>99</sup>Mo producers for a certain production output

needed for customer demands. So, taking it one step further, a target which minimises both the amount of  $^{235}\text{U}$  burned up and considers the need for  $^{99}\text{Mo}$  total output ( $A_T$ ), can be expressed by a parameter termed ‘target quality’ or  $Q_{\text{targ}}$ , where:

$$Q_{\text{targ}} = \epsilon'_{\text{targ}} \times A_T \left( \text{GBq}^2 \cdot \text{g}^{-1} \right) \tag{4}$$

Thus, a target with a high  $Q_{\text{targ}}$  would produce the highest  $^{99}\text{Mo}$  output for the  $^{235}\text{U}$  burned. However, it does not tell us about the remaining  $^{235}\text{U}$  left in the target which would naturally be in excess therefore, it is desirable to consider the total amount of  $^{235}\text{U}$  originally in the target before irradiation,  $^{235}\text{U}_T$ , because the amount remaining in the target after the target’s use should—all things being equal—be minimized, so a target with a lower  $^{235}\text{U}_T$  would be superior. Hence, a target sustainability index  $S_{\text{targ}}$  is proposed, where:

$$\begin{aligned} S_{\text{targ}} &= \frac{\epsilon'_{\text{targ}} A_T}{^{235}\text{U}_T} \\ &= \frac{Q_{\text{targ}}}{^{235}\text{U}_T} \\ &= \frac{A_T^2}{^{235}\text{U}_T \cdot ^{235}\text{U}_b} \left( \text{Bq}^2 \cdot \text{g}^{-2} \right) \end{aligned} \tag{5}$$

where  $A_T$  is a predefined amount of  $^{99}\text{Mo}$  desired to be produced in the irradiation,  $^{235}\text{U}_T$  is the total amount of  $^{235}\text{U}$  in the target before the irradiation, and  $^{235}\text{U}_b$  is the amount of  $^{235}\text{U}$  burned up in the irradiation [32]. The sustainability index was used previously in the modelling of the targets to compare how different variables in target composition, geometry and irradiation times affect the amount of waste produced by the targets after irradiation.

Four different theoretical targets were designed to give a  $^{99}\text{Mo}$  output of approximately 9000 GBq based on cylindrical geometry as it was found that cylindrical geometry leads to an optimal sustainability index and  $^{99}\text{Mo}$  output [33]. The target dimensions are given in Table 2 and the targets were in the vertical orientation which was the same as the reactor core to maximise neutron interactions. The targets were placed in the middle of the horizontal plane of the reactor core also to maximise neutron interactions. The output target of 9000 GBq of  $^{99}\text{Mo}$  was based on a small  $^{99}\text{Mo}$  producer for proof of concept to give a weekly output of approximately 37,000 GBq (1000 Ci) if 4 runs per week were completed, which is an indicative of a size of a regional producer [36]. For larger producers increased output can be obtained by increasing target volume whilst maintaining constant density [33]. Consistent with previous research [34], irradiation times of 4–7 days were used as this was found to be the optimal irradiation times for maximising the sustainability index of the targets.

**Table 2.** Geometry of 4 different targets to produce approximately 9000 GBq.

Target Number	Irradiation Time (Days)	Shape	Height (cm)	Radius (cm)	Volume (cm <sup>3</sup> )	<sup>235</sup> U (grams)
1	4	cylinder	10.4	1.13	41.72	0.7593
2	5		9	1.13	36.10	0.6570
3	6		8.2	1.13	32.89	0.5986
4	7		7.8	1.13	31.29	0.5695

The number of initial neutrons for the simulations was set to 50,000 as this was previously found to contain relatively low errors, compared to using a lower number of initial neutrons. The target modelled in this study was a 1% enriched  $\text{UO}_2$  target as this was found to have the highest sustainability index compared to using targets in the enrichment range of 3–20% [32]. Targets were modelled for sustainability index,  $^{99}\text{Mo}$  output and  $^{239}\text{Pu}$  levels to determine if changing the material of the target has any effect on these values.  $^{239}\text{Pu}$  levels in the burnt-up targets were compared against the amount of  $^{239}\text{Pu}$  required to produce 1 bare critical mass (BCM) which is 10.4 kg and of proliferation concern [3]. Previously [32,36] the amount of  $^{239}\text{Pu}$  produced in the target after irradiation

was normalised to determine how many 100,000 GBq runs are required to produce 10.4 kg of  $^{239}\text{Pu}$  and in this study the same approach was used. Due to  $^{140}\text{Ce}$  not undergoing fission reactions and forming any uranium isotopes, it is expected that there will be very little to no change on the sustainability index or the  $^{99}\text{Mo}$  output but a noticeable reduction in  $^{239}\text{Pu}$  levels post irradiation due to lowering the amount of  $^{238}\text{U}$  in the target.

MCNP6.2 [31] can also determine the heating of materials that undergo interactions with neutrons via the “F6 heating tally” function. The F6 heating tally uses the probability of neutron interaction and neutron energies to calculate the energy deposited in the material in MeV/g [37]. The heating of the target’s during irradiation was examined using the F6 tally to determine if the addition of Ce would cause a problem due to targets obtaining excess heat and this was compared to previous work on target heating in a pure  $\text{UO}_2$  target [33]. Typically, LEU targets produce a considerable amount of heat and so are designed for this to be quickly dissipated during irradiation.

### 2.3. Errors in Graphs

MCNP6.2 [31] is known to have small statistical errors in its calculations. These errors have been found to be less than 5% for low levels of burnup [38]. Since it is expected that the addition of Ce in the target composition will have no effect on the  $^{99}\text{Mo}$  output or the sustainability index of the 4 target types, the data provided by the simulations is thought to produce a horizontal line, i.e., no difference as Ce levels increase and  $^{238}\text{U}$  levels decrease. Errors in sustainability index and  $^{99}\text{Mo}$  output were therefore calculated by the following formula:

$$E(\%) = \left( \frac{\text{Value} - \text{Average}}{\text{Average}} \right) \times 100 \quad (6)$$

where  $E(\%)$  is error, value is the result from the simulation and average is the result from the 11 values for that target from the simulation. This error calculation was applied to all 4 targets and displayed in error bars on the figures.

### 2.4. Target Radius

To determine the effects of increasing the target radius whilst maintaining a consistent target height, targets with height of 10 cm and radius 1–3 cm (with increments of 0.1 cm in radius) were modelled. Target volumes versus radius can be seen in Figure 2. The target model was based on an example consisting of 20% enriched uranium blended with  $^{140}\text{Ce}$  to down blend the uranium to 1% enriched. In this case, the target composition is 95%  $^{140}\text{Ce}$ , 4%  $^{238}\text{U}$  and 1%  $^{235}\text{U}$ .

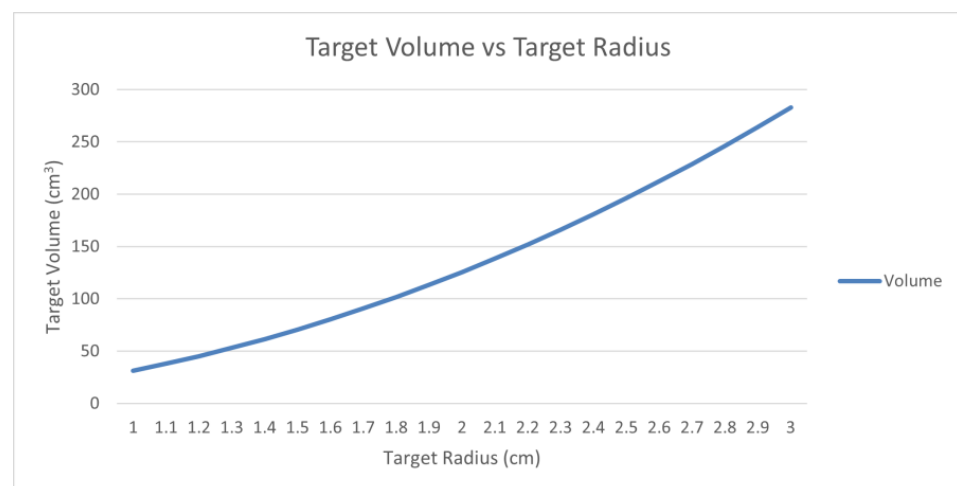


**Figure 2.** 1% enriched target with height 10 cm and target volume compared to radius plotted.

### 3. Results

The sustainability index was examined for the CeO<sub>2</sub>-UO<sub>2</sub> targets 1–4 as shown in Figure 3.

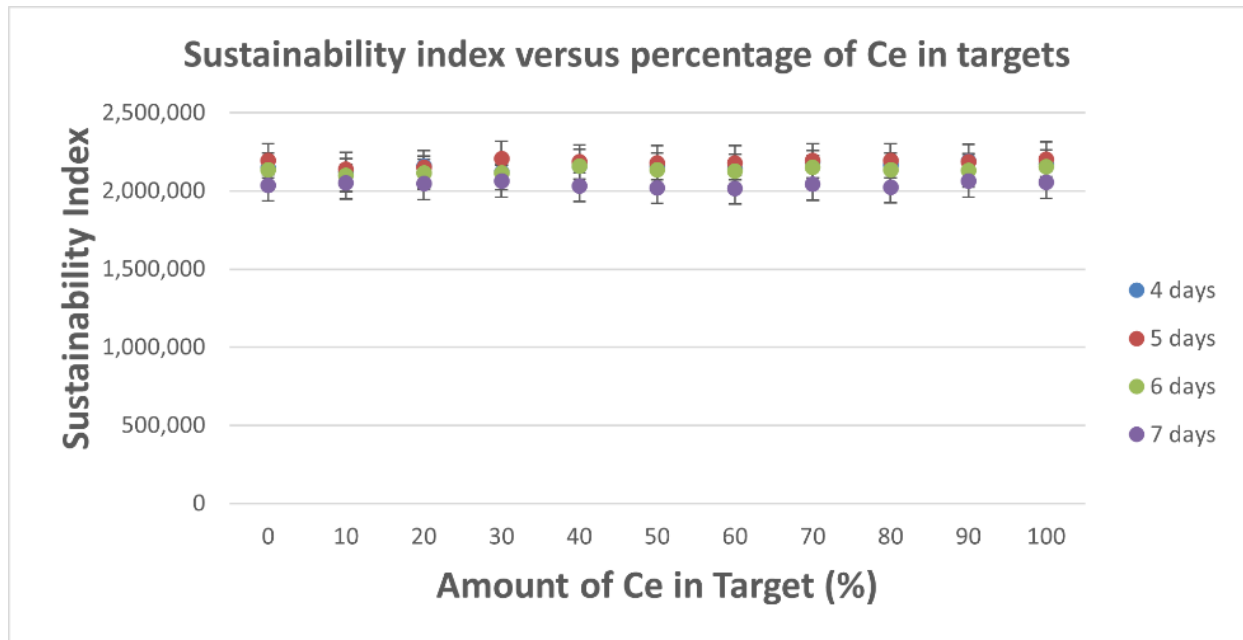


Figure 3. How the sustainability index varies with increasing amount of Ce in targets with 4 days irradiation.

The <sup>99</sup>Mo output of the 4 target types is given in Figure 4.

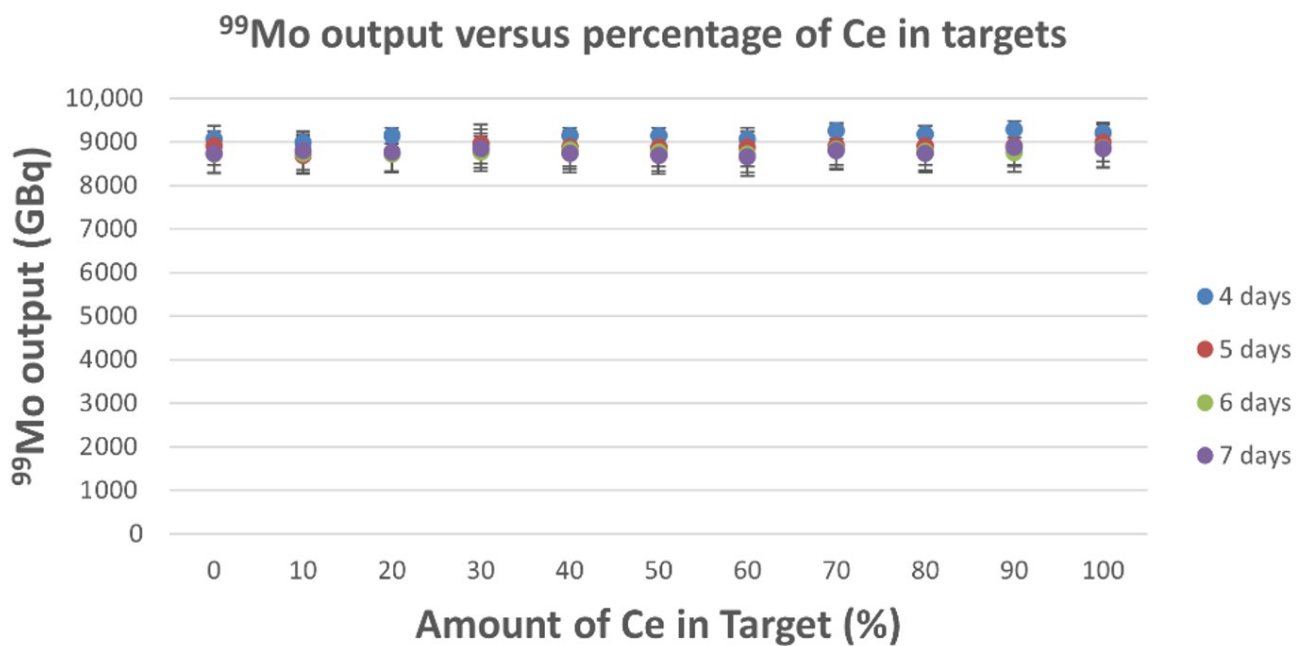


Figure 4. <sup>99</sup>Mo output of 4 target types with varying amount of Ce.

The number of 100,000 GBq production runs to produce 10.4 kg <sup>239</sup>Pu for each of the four target types is plotted in Figure 5.

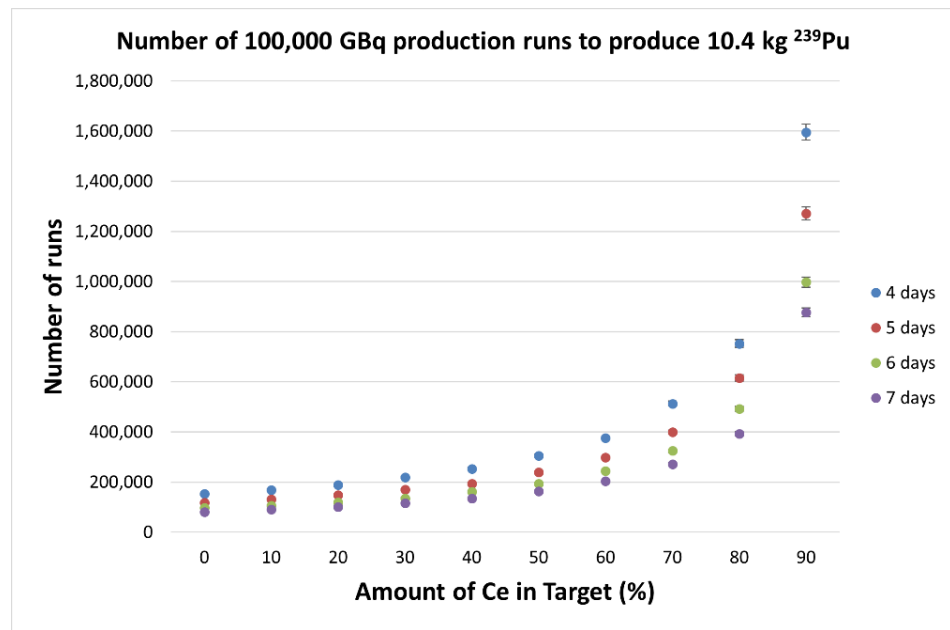


Figure 5. Comparative <sup>239</sup>Pu levels in targets with varying amounts of Ce.

The heating tallies of the four target types is given in Table 3.

Table 3. Results of F6 heating tallies for 4 target types.

Target Type	Average Heat (MeV/g)	Average Relative Error
1	$3.13 \times 10^{-4}$	$3.60 \times 10^{-3}$
2	$3.12 \times 10^{-4}$	$3.80 \times 10^{-3}$
3	$3.09 \times 10^{-4}$	$3.83 \times 10^{-3}$
4	$3.07 \times 10^{-4}$	$4.00 \times 10^{-3}$

Changes in Radius

Figures 6–8 show the effects of changes in target radius for a fixed height target on <sup>99</sup>Mo output, sustainability index and <sup>239</sup>Pu levels produced in the targets.

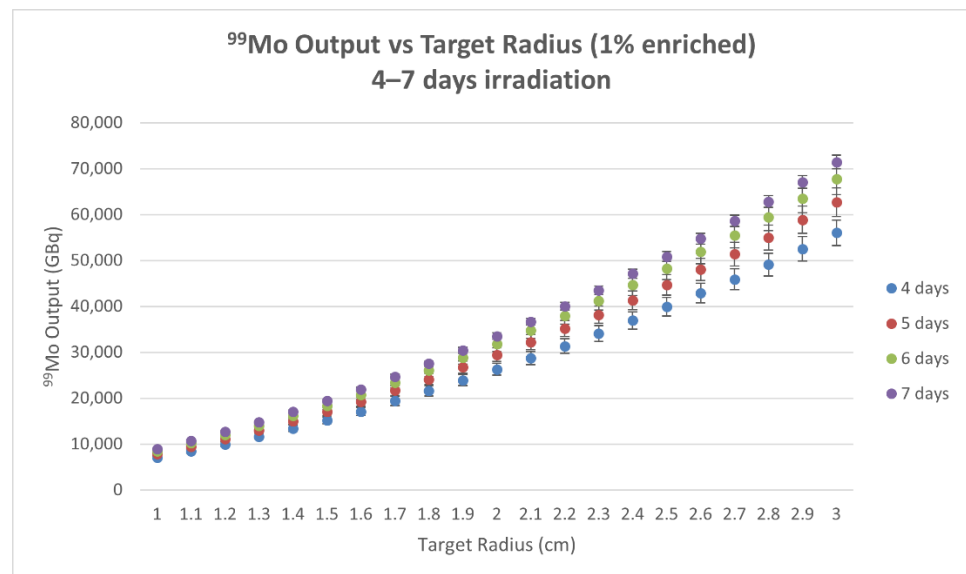


Figure 6. <sup>99</sup>Mo output versus target radius for a fixed target height of 10 cm.

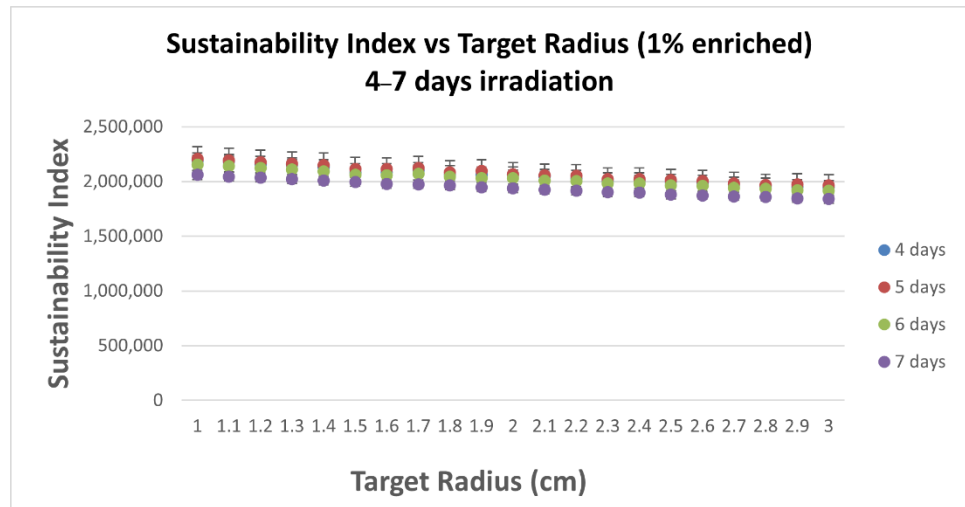


Figure 7. Sustainability index versus target radius for a fixed target height of 10 cm.

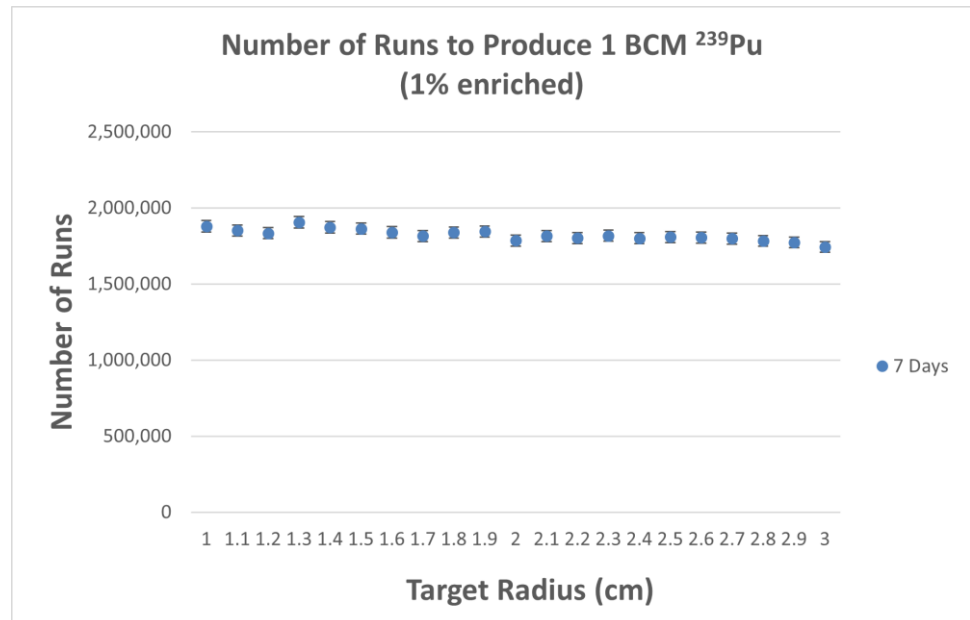


Figure 8. Number of runs to produce 1 BCM of <sup>239</sup>Pu versus target radius for a fixed target height of 10 cm.

#### 4. Discussion

The objective of this study was to determine if the replacement of <sup>238</sup>U with <sup>140</sup>Ce would have any detrimental effect on the sustainability index or <sup>99</sup>Mo output of 4 different targets configurations and any positive effect on the <sup>239</sup>Pu levels produced in the target. For targets 1–4, Figures 2 and 3 show that the sustainability index and <sup>99</sup>Mo output are relatively the same for all amounts of <sup>140</sup>Ce percentage from 0% up to 99% which was to be expected. Figures 2 and 3 also highlight the combinations of variables that can go into a target to produce similar output such as material composition, geometry and irradiation time which were all varied to produce approximately 9000 GBq of <sup>99</sup>Mo which is the amount of a regional producer. The factor that remained constant was that 1% enriched cylindrical targets were used. The errors in the results were within the accepted levels that are produced by MCNP6.2 [31,38].

Figure 4 shows how many 100,000 GBq production runs it takes to produce 1 BCM of <sup>239</sup>Pu. When the ratio of Ce in the target is low approximately 100,000 production runs

are possible before reaching 1 BCM, however as the ratio of Ce in the target increases the number of runs it takes to produce 1 BCM increases exponentially to over 1,000,000 production runs needed which is a ten-fold increase. Figure 9 compares the number of 100,000 GBq production runs to produce 1 BCM of  $^{239}\text{Pu}$  with previous research done on pure  $^{238}\text{U}/^{235}\text{U}$  targets [33].

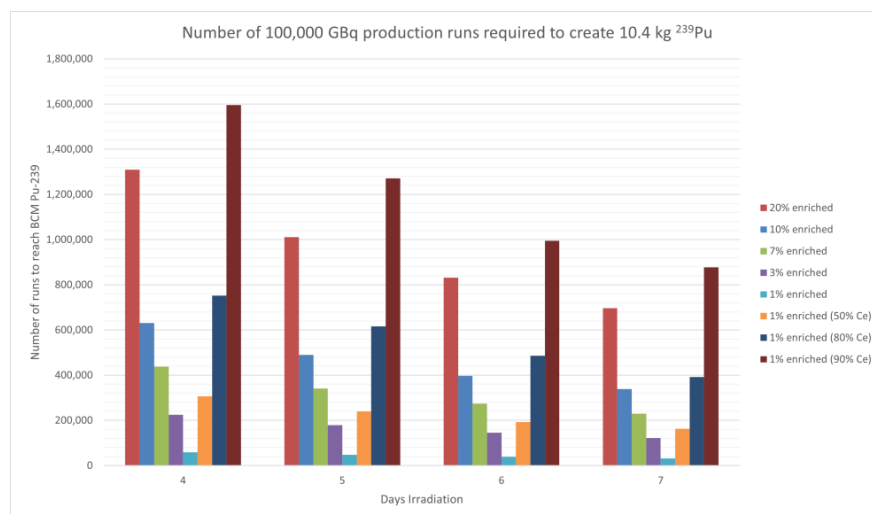


**Figure 9.** Comparison of number of 100,000 GBq runs to produce 1 BCM of  $^{239}\text{Pu}$  with different enrichment levels in [32] compared with 50% and 90% Ce added to the target.

It was expected that  $^{239}\text{Pu}$  levels increase in targets with lower enrichment as a previous study found a 50-fold increase in  $^{239}\text{Pu}$  levels when comparing HEU and LEU [39] and higher levels of  $^{239}\text{Pu}$  were found in lower enriched targets in the simulation. Figure 8 shows that the substitution of  $^{238}\text{U}$  with  $^{140}\text{Ce}$  offsets this disadvantage and leads to the number of production runs for the 50% Ce target to be higher than for a 3% enriched target, and for a 90% Ce target the number of production runs is even higher than that of the 20% enriched target which means that the 90% Ce target is a much lower proliferation risk compared to the 20% LEU targets currently being used when normalised for  $^{99}\text{Mo}$  output of 100,000 GBq due to the removal of  $^{238}\text{U}$  in the target.

Table 3 indicates that there is no issue with the addition of Ce into the target in terms of target heating as the highest average target heat was found to be  $3.13 \times 10^{-4}$  MeV/g which is comparable to the pure  $\text{UO}_2$  targets modelled previously [33].

Figure 6 shows that the amount of  $^{99}\text{Mo}$  output in the target can also be increased by increasing the target radius as the output increases consistently with increasing target radius. Another study on a uranyl nitrate solution  $^{99}\text{Mo}$  production method that used MCNP to model natural uranium found that the  $^{99}\text{Mo}$  output doubled when the amount of  $^{235}\text{U}$  in the solution was doubled [40]. When the target volume was doubled in this study by increasing the radius of the target the  $^{99}\text{Mo}$  output also doubled which agrees with the uranyl nitrate study.

The sustainability index shown in Figure 7 displays a small decrease as target radius increases which does indicate a small loss in efficiency as target radius increases and this difference can be attributed to the increasing effects of self-shielding as to be expected when increasing the thickness of the target. Looking at Figure 8 the amount of 100,000 GBq runs decreases as the target radius increases also indicating a loss of target efficiency, though with over 1 million runs to produce 1 BCM of  $^{239}\text{Pu}$  a larger  $^{99}\text{Mo}$  producer might be willing to trade off the much larger  $^{99}\text{Mo}$  output against the slightly less target sustainability.

## 5. Conclusions

In addition to modifying target geometry and enrichment, this study also demonstrates that the composition of the target can be changed from  $^{238}\text{U}$  to Ce whilst maintaining a

high sustainability index, a predictable  $^{99}\text{Mo}$  output, and lowering the amounts of  $^{239}\text{Pu}$  present in the target after irradiation. This would also present a significant cost saving to the target user due to much lower (1/100th) of the cost of cerium oxide versus uranium oxide. The heating in the  $\text{CeO}_2\text{-UO}_2$  target was also found to be comparable to the pure  $\text{UO}_2$  target. This study has expanded the possibility for uranium target designs that could allow for more flexibility in the parameters used and this could lead to less production and waste compared to a 100% uranium-based target. Some example applications of the ability to alter the material composition could be target manufacturers who possess 20% enriched uranium could make up a target of 5% of this uranium and 95% Ce to get a  $^{235}\text{U}$  content of 1% in the mixture to produce a highly sustainable target whilst at the same time reducing the world supply of enriched uranium instead of having to continue enriching natural uranium for target creation and burn it up the more traditional way. A larger  $^{99}\text{Mo}$  producer might be able to modify the target radius to suit production requirements as this was shown to increase output at the cost of a slightly reduced target sustainability and slightly more  $^{239}\text{Pu}$  production.

**Author Contributions:** Conceptualization, R.R. and G.T.; methodology, R.R. and J.B.-W.; software, R.R.; validation, G.T.; formal analysis, R.R. and G.T.; investigation, R.R. and G.T.; resources, R.R. and G.T.; data curation, R.R.; writing—original draft preparation, R.R. and G.T.; writing—review and editing, R.R., A.R. and G.T.; visualization, R.R.; supervision A.R. and G.T. All authors have read and agreed to the published version of the manuscript.

**Funding:** This research received no external funding.

**Data Availability Statement:** Not applicable.

**Conflicts of Interest:** The authors declare no conflict of interest.

## References

1. Hassan, M.u.; Ryu, H.J. Radioactive Waste Issues Related to Production of Fission-based  $^{99}\text{Mo}$  by using Low Enriched Uranium (LEU). *J. Nucl. Fuel Cycle Waste Technol.* **2015**, *13*, 155–161. Available online: <http://www.jnfcwt.or.kr/journal/article.php?code=31995> (accessed on 2 June 2022). [CrossRef]
2. Lyman, E.S. Excess Plutonium Disposition: The Failure of MOX and the Promise of Its Alternatives. 2014. Available online: [www.ucsusa.org/our-work/nuclear/](http://www.ucsusa.org/our-work/nuclear/) (accessed on 2 June 2022).
3. Glaser, A. About the Enrichment Limit for Research Reactor Conversion: Why 20%? In Proceedings of the 27th International Meeting on Reduced Enrichment for Research and Test Reactors (RERTR), Boston, MA, USA, 6–10 November 2005.
4. Albright, D.; Kelleher-Vergantini, S. *Plutonium and Highly Enriched Uranium 2015 Military Highly Enriched Uranium and Plutonium Stocks in Acknowledged Nuclear Weapon States a End of 2014*; Institute for Science and International Security: Washington, DC, USA, 16 November 2015.
5. Betti, M. Civil use of depleted uranium. *J. Environ. Radioact.* **2003**, *64*, 113–119. Available online: [www.elsevier.com/locate/jenvrad](http://www.elsevier.com/locate/jenvrad) (accessed on 9 June 2022). [CrossRef]
6. Foral, Š.; Salamon, D.; Katovský, K.; Varmuža, J.; Roleček, J. Influence of Silicone Carbide on the Reactivity of Nuclear Fuels Using Cerium Dioxide as a Surrogate Material. In *Innovative Nuclear Power Plant Design and New Technology Application*; Student Paper Competition; American Society of Mechanical Engineers: New York, NY, USA, 2014; Volume 5.
7. Roleček, J. A feasibility study of using  $\text{CeO}_2$  as a surrogate material during the investigation of  $\text{UO}_2$  thermal conductivity enhancement. *Adv. Appl. Ceram.* **2017**, *116*, 123. [CrossRef]
8. Valderrama, B.; Henderson, H.; He, L.; Yablinsky, C.; Gan, J.; Hassan, A.-R.; El-Azab, A.; Allen, T.; Manuel, M. Fission Products in Nuclear Fuel: Comparison of Simulated Distribution with Correlative Characterization Techniques. *Microsc. Microanal.* **2013**, *19*, 968–969. [CrossRef]
9. Lee, Y.W.; Lee, S.C.; Joung, C.Y.; Kim, H.S.; Lee, H.L. Analysis of resistance to thermal stress in ceramic oxide nuclear materials. *Adv. Eng. Mater.* **2002**, *4*, 584–589. [CrossRef]
10. Lantz, P.M.; Baldock, C.R.; Idom, L.E. Thermal-Neutron Capture Cross Section and Resonance Capture Integral of  $\text{Ce}^{140}$  and Effective Capture Cross Section of  $\text{Ce}^{141}$ . *Nucl. Sci. Eng.* **1964**, *20*, 302–306. [CrossRef]
11. Torrel, S.; Krane, K.S. Neutron capture cross sections of  $^{136,138,140,142}\text{Ce}$  and the decays of  $^{137}\text{Ce}$ . *Phys. Rev. C-Nucl. Phys.* **2012**, *86*, 034340. [CrossRef]
12. Nelson, A.T.; Rittman, D.R.; White, J.T.; Dunwoody, J.T.; Kato, M.; McClellan, K.J. An Evaluation of the Thermophysical Properties of Stoichiometric  $\text{CeO}_2$  in Comparison to  $\text{UO}_2$  and  $\text{PuO}_2$ . *J. Am. Ceram. Soc.* **2014**, *97*, 3652–3659. [CrossRef]
13. Lu, P.; Qiao, B.; Lu, N.; Hyun, D.C.; Wang, J.; Kim, M.J.; Liu, J.; Xia, Y. Photochemical Deposition of Highly Dispersed Pt Nanoparticles on Porous  $\text{CeO}_2$  Nanofibers for the Water-Gas Shift Reaction. *Adv. Funct. Mater.* **2015**, *25*, 4153–4162. [CrossRef]

14. Magneli, A.; Kihlberg, L. *acta\_vol\_05\_p0578-0580. Acta Chem. Scand.* **1951**, *5*, 578–580.
15. Lee, D.W.; Lee, J.; Kim, J.Y.; Lim, S.H. Influence of Ce (III) Cation on Structural Property of Uranium Dioxide. In Proceedings of the Transactions of the Korean Nuclear Society Spring Meeting, Jeju, Korea, 22 May 2019.
16. Guo, X.; Navrotsky, A.; Shvareva, T.; Rock, P.A. *Thermodynamics of Uranium Minerals and Related Materials Chapter 4: Thermodynamics of Uranium Minerals and Related Materials*; Mineralogical Association of Canada: Winnipeg, MB, Canada, 2013.
17. Brilliant, G.; Gupta, F.; Pasturel, A. Fission products stability in uranium dioxide. *J. Nucl. Mater.* **2011**, *412*, 170–176. [[CrossRef](#)]
18. Iwasawa, M.; Ohnuma, T.; Chen, Y.; Kaneta, Y.; Geng, H.-Y.; Iwase, A.; Kinoshita, M. First-principles study on cerium ion behavior in irradiated cerium dioxide. *J. Nucl. Mater.* **2009**, *393*, 321–327. [[CrossRef](#)]
19. Mihara, T.; Abe, H.; Iwai, T.; Sonoda, T.; Wakai, E. Microstructural Evolution in Cerium Dioxide Irradiated with Heavy Ions at High Temperature. In Proceedings of the Joint International Workshop: Nuclear Technology and Society—Needs for Next Generation, Berkeley, CA, USA, 6–8 January 2008.
20. Stennett, M.C.; Corkhill, C.L.; Marshall, L.A.; Hyatt, N.C. Preparation, characterisation and dissolution of a CeO<sub>2</sub> analogue for UO<sub>2</sub> nuclear fuel. *J. Nucl. Mater.* **2013**, *432*, 182–188. [[CrossRef](#)]
21. Aidhy, D.S.; Wolf, D.; El-Azab, A. Comparison of point-defect clustering in irradiated CeO<sub>2</sub> and UO<sub>2</sub>: A unified view from molecular dynamics simulations and experiments. *Scr. Mater.* **2011**, *65*, 867–870. [[CrossRef](#)]
22. Ye, B.; Oaks, A.; Kirk, M.; Yun, D.; Chen, W.-Y.; Holtzman, B.; Stubbins, J.F. Irradiation effects in UO<sub>2</sub> and CeO<sub>2</sub>. *J. Nucl. Mater.* **2013**, *441*, 525–529. [[CrossRef](#)]
23. Zhang, Y.; Hansen, E.D.; Harbison, T.; Masengale, S.; French, J.; Aagesen, L. A molecular dynamics survey of grain boundary energy in uranium dioxide and cerium dioxide. *J. Am. Ceram. Soc.* **2022**, *105*, 4471–4486. [[CrossRef](#)]
24. Devanathan, R. Molecular Dynamics Simulation of Fission Fragment Damage in Nuclear Fuel and Surrogate Material. *MRS Adv.* **2017**, *2*, 1225–1230. [[CrossRef](#)]
25. Frazer, D.; Maiorov, B.; Carvajal-Nuñez, U.; Evans, J.; Kardoulaki, E.; Dunwoody, J.; Saleh, T.; White, J. High temperature mechanical properties of fluorite crystal structured materials (CeO<sub>2</sub>, ThO<sub>2</sub>, and UO<sub>2</sub>) and advanced accident tolerant fuels (U<sub>3</sub>Si<sub>2</sub>, UN, and UB<sub>2</sub>). *J. Nucl. Mater.* **2021**, *554*, 153035. [[CrossRef](#)]
26. Patnaik, S. Comparative analysis of temperature dependent properties of commercial nuclear fuel pellet and surrogates undergoing cracking: A review. *Ceram. Int.* **2020**, *46*, 24765–24778. [[CrossRef](#)]
27. Weber, M.H.; McCloy, J.S.; Halverson, C.R.; Karcher, S.E.; Mohun, R.; Corkhill, C.L. Characterization of vacancy type defects in irradiated UO<sub>2</sub> and CeO<sub>2</sub>. *MRS Adv.* **2022**, *7*, 123–127. [[CrossRef](#)]
28. Lee, S.C.; Lee, H.R.; Joung, C.Y.; Lee, Y.W. Effect of microstructure on the fracture properties of UO<sub>2</sub>-5wt%CeO<sub>2</sub> Pellets. *J. Nucl. Sci. Technol.* **2002**, *39*, 819–822. [[CrossRef](#)]
29. Shanghai Metals Market. 2022. Available online: <https://www.metal.com/price/Rare%20Earth/Rare-Earth-Oxides> (accessed on 1 August 2022).
30. Wulandari, F. Capital.com. 2022. Available online: <https://capital.com/uranium-price-forecast#:~:text=In%20his%20uranium%20price%20projections%2C%20David%20Talbot%20of,not%20provide%20a%20uranium%20price%20forecast%20for%202030> (accessed on 1 August 2022).
31. Werner, C.J.; Bull, J.S.; Solomon, C.J.; Brown, F.B.; McKinney, G.W.; Rising, M.E.; Dixon, D.A.; Martz, R.L.; Hughes, H.G.; Cox, L.J.; et al. *MCNP Version 6.2 Release Notes*; Los Alamos National Laboratory: Los Alamos, NM, USA, 2018.
32. Raposio, R.; Braoudakis, G.; Rosenfeld, A.; Thorogood, G.J.; Bedwell-Wilson, J. Investigating an alternative sustainable low enriched uranium target for the manufacture of <sup>99</sup>Mo using MCNP6.2 modelling with CINDER90. *Front. Nucl. Eng.* (In press).
33. Raposio, R.; Braoudakis, G.; Rosenfeld, A.; Thorogood, G. Investigating <sup>99</sup>Mo output changes in high sustainability uranium targets by modifying target volume and geometry. *Front. Nucl. Eng.* (In press).
34. Raposio, R.; Braoudakis, G.; Rosenfeld, A.; Thorogood, G.J. Modelling of reusable target materials for the production of fission produced <sup>99</sup>Mo using MCNP6.2 and CINDER90. *Appl. Radiat. Isot.* **2021**, *176*, 109827. [[CrossRef](#)]
35. National Research Council. *Medical Isotope Production without Highly Enriched Uranium*; National Academies Press: Washington, DC, USA, 2009; pp. 1–220.
36. Katcoff, S.; Leary, J.A.; Walsh, K.A.; Elmer, R.A.; Goldsmith, S.S.; Hall, L.D.; Newbury, E.G.; Povelites, J.J.; Waddell, J.S. Neutron absorption cross sections of radioactive La<sup>140</sup> and two stable cerium isotopes. *J. Chem. Phys.* **1948**, *17*, 421–424. [[CrossRef](#)]
37. X-5 Monte Carlo Team. *MCNP—A general Monte Carlo N-Particle Transport Code, Version 5*; LA-UR-0-1987; Los Alamos National Laboratory: Los Alamos, NM, USA, 2008; pp. 1–416.
38. García-Herranz, N.; Cabellos, O.; Sanz, J. Assessment of the MCNP-ACAB code system for burnup credit analyses. In Proceedings of the International Workshop in Advances in Applications of Burnup Credit for Spent Fuel Storage, Transport, Reprocessing, and Disposition, Cordoba, Spain, 27–30 October 2009.
39. Cho, D.-K.; Kim, M.-H. Performance Uncertainties of LEU Mo-99 targets for HANARO. In Proceedings of the International Meeting on Reduced Enrichment for Research and Test Reactors, Bariloche, Argentina, 3–8 November 2002.
40. Verner, K.M.; Kim, S.J. Molybdenum-99 production via fissile solution reactor and electron beam accelerator. In Proceedings of the ANS Winter Conference Meeting, Washington, DC, USA, 9–13 June 2019.